Katholieke Universiteit Leuven

Departement Elektrotechniek

ESAT-SISTA/TR 03-36

Nonparametric Regularized Time Delay Estimation[1]

Oscar Barrero Mendoza and Bart De Moor[2]

August 22, 2003

[1]This report is available by anonymous ftp from *ftp.esat.kuleuven.ac.be* in the directory *pub/sista/barrero/reports/NPTDelay.ps.gz*

[2]Dr. Bart De Moor is a full professor at the Katholieke Universiteit Leuven, Belgium. Research supported by Research Council KUL: GOA-Mefisto 666, several PhD/postdoc fellow grants; Flemish Government: - FWO: PhD/postdoc grants, projects, G.0240.99 (multilinear algebra), G.0407.02 (support vector machines), G.0197.02 (power islands), G.0141.03 (Identification and cryptography), G.0491.03 (control for intensive care glycemia), G.0120.03 (QIT), research communities (ICCoS, ANMMM); - AWI: Bil. Int. Collaboration Hungary/ Poland; - IWT: PhD Grants, Soft4s (softsensors), Belgian Federal Government: DWTC (IUAP IV-02 (1996-2001) and IUAP V-22 (2002-2006), PODO-II (CP/40: TMS and Sustainibility); EU: CAGE; ERNSI; Eureka 2063-IMPACT; Eureka 2419-FliTE; Contract Research/agreements: Data4s, Electrabel, Elia, LMS, IPCOS, VIB

Abstract

In this paper a novel non-parametric estimator, which we call the Regularized Time Delay Estimator (RTDE), is introduced for the time delay estimation problem in MISO (Multiple Input-Single Output) linear systems. This estimator decouples the input-output signals in the frequency domain using a regularized Wiener-Hopf filter. An RLS (Regularized Least Squares [5]) problem is formulated based on the coherence spectrum in order to find the optimal filter that can decouple the signals. Then, the corresponding delayed impulse responses of the system are computed. Thus, time delay between the several input-output signals can be estimated independently.

Keywords: Signal Preprocessing, Coherence Spectrum, Cross Power Spectrum, Regularized Least Squares.

1 Introduction

As a consequence of industrial automation, many process industry companies like to exploit the enormous and valuable data they have recorded from Data Acquisition Systems to build models of their processes. Although today several methods exist to build models based on data, there are still many problems to be solved, one of which is time delay estimation. In this paper, the problem of time delay estimation for MISO (Multiple Inputs - Single Outputs) systems based on noisy measured data is treated.

When dealing with data preprocessing for modelling process, the problem of measuring variables with a time delay is very often encountered. As a motivation, let's consider the measurement of the flow rate at the beginning of a pipeline. Often it is not possible to install the sensor in a desired location due to problems such as high local temperatures and/or pressures, .. etc. It is necessary to install the sensors in some remote safe place, with as a consequence that there is a delay in observing the variable. Then, if we want to use these observations to perform a linear model identification, for instance, the computation will be harder due to the fact that time delays introduce extra parameters to be estimated into the model. In addition, the estimation of time delays as part of the model does not contribute to the further description of the dynamic behaviour of the process. Hence, it is recommended to estimate time delays separate from the model dynamics as a kind of preprocessing step.

Basically, there are two methodologies to solve the problem. The first one is model-based or parametric estimation, where some assumptions have to be made about the system dynamics, and the second one is model-independent or nonparametric estimation, where the estimation is done based on the analysis of the data.

In this work, we will focus on the nonparametric case. In the literature, some classical methods for time delay estimation based on the technique of cross-correlation are found (see [6], [3], [1]). Although, they have been shown to work pretty well, they were basically designed to deal with SISO (Single Input - Single Output) systems. Hence, some extra considerations like input signal decoupling have to be done in order to extend these methods to the MISO (Multiple Inputs - Multiple Outputs) case. As a result, a new time delay estimator for MISO systems based on generalized cross-correlation is introduced in this paper, which will be called Regularized Time Delay Estimator (RTDE). This estimator decouples the input-output signals in the frequency domain using Wiener-Hopf filter which is regularized by the coherence spectrum (see 2.2). Therefore, an RLS (Regularized Least Squares [5]) problem is formulated based on the coherence spectrum such that this filter is able to decouple the signals in an optimal way. Consequently, the corresponding delayed impulse responses and time delays of the system are computed.

This paper is organized as follows: In Section 1, some relevant concepts are presented. In Section 2, the problem formulation is given. In Section 3, the RTDE approach for time delay estimation of MISO systems is introduced. In Section 4, some numerical results are showed. Finally, Section 5 gives some

concluding remarks.

2 Some Definitions

2.1 Cross-Correlation function

The Cross-Correlation function between two signals $u(k)$ and $y(k)$ in the discrete time domain is defined as

$$R_{uy}(\tau) = E[u(k+\tau)y(k)], \qquad -\infty < k < \infty, \ -T < \tau < T \tag{1}$$

where $E[\cdot]$ denotes the mathematical expectation.

Applying the DTFT (Discrete Time Fourier Transform) to (1), gives

$$G_{uy}(e^{j\omega}) = Y(e^{j\omega})U^*(e^{j\omega}), \tag{2}$$

where '*' denotes conjugate, $Y(e^{j\omega})$ and $U(e^{j\omega})$ are the DTFT of $y(k)$ and $u(k)$, and $G_{uy}(e^{j\omega})$ is the *Cross-Power Spectrum*.

Now, we can express the output of a SISO linear system as a function of the impulse response $h(k)$ as follows

$$y(k) = h(k) * u(k), \tag{3}$$

where '$*$' denotes convolution, then, by applying the DTFT we have

$$Y(e^{j\omega}) = H(e^{j\omega})U(e^{j\omega}) \tag{4}$$

Replacing (4) in (2) we can rewrite the cross-power spectrum as

$$G_{uy}(e^{j\omega}) = H(e^{j\omega})U(e^{j\omega})U^*(e^{j\omega}) \tag{5}$$

2.2 Coherence Spectrum

The coherence spectrum between two signals $u(k)$ and $y(k)$ is equal to the cross power spectrum $G_{uy}(e^{j\omega})$ divided by the square root of the product of the two auto power spectra. Specifically, the complex coherence is defined by

$$\gamma_{uy}(e^{j\omega}) = \frac{G_{uy}(e^{j\omega})}{\sqrt{G_{uu}(e^{j\omega})G_{yy}(e^{j\omega})}}. \tag{6}$$

where $G_{uy}(e^{j\omega})$ is the Fourier transform of the cross correlation function (see equation (1)).
The coherence is a normalized cross-spectral density function; in particular, the normalization constrains so that the magnitude-squared coherence (MSC) defined by

$$C_{uy}(e^{j\omega}) \triangleq |\gamma_{uy}(e^{j\omega})|^2 \tag{7}$$

lies in the range $0 \leq C_{uy}(e^{j\omega}) \leq 1$, for all frequencies ω.

The coherence function has been used in numerous areas including system identification, measurement of signal to noise-ratio (SNR), and determination of time delay. The coherence -in particular, magnitude-squared coherence (MSC)- can only be put to use when its value can be accurately estimated. Indeed, it is highly desirable to understand the statistics of the estimator.

One interesting interpretation of coherence -particularly MSC- is that it is a measure of the relative linearity of two processes. To illustrate this, consider fig. 1 in which a sample function $y(k)$ of an arbitrary stationary random process consists of the response $y_0(k)$ of a linear filter plus an error component $e(k)$. When the linear filter is chosen to minimize the mean-square value of $e(k)$, i.e.,

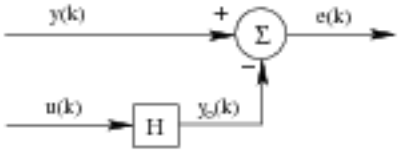


Figure 1: Model of error resulting from linearly filtering $u(k)$ to match any desired signal $y(k)$.

the area under the error spectrum, then $y_0(k)$ becomes that part of $y(k)$ linearly related to $u(k)$. The spectral characteristics of $e(k)$ are given by

$$G_{ee}(e^{j\omega}) = G_{yy}(e^{j\omega}) + G_{uu}(e^{j\omega})|H(e^{j\omega})|^2 - H(e^{j\omega})G^*_{uy}(e^{j\omega}) - H^*(e^{j\omega})G_{uy}(e^{j\omega}) \tag{8}$$

where * indicates complex conjugation and $H(e^{j\omega})$ is the filter transfer function. The error spectrum

$$G_{ee}(e^{j\omega}) = G_{uu}(e^{j\omega})\left|H(e^{j\omega}) - \frac{G_{ug}(e^{j\omega})}{G_{uu}(e^{j\omega})}\right|^2 + G_{gg}(e^{j\omega})[1 - C_{uy}(e^{j\omega})|. \tag{9}$$

Hence, the optimum filter is given by

$$H_0(e^{j\omega}) = \frac{G_{ug}(e^{j\omega})}{G_{uu}(e^{j\omega})}. \tag{10}$$

Note that the coherence is related to the optimum linear filter according to

$$\gamma(e^{j\omega}) = H_0(e^{j\omega})\sqrt{\frac{G_{uu}(e^{j\omega})}{G_{yg}(e^{j\omega})}} \tag{11}$$

and

$$C_{uy}(e^{j\omega}) = |H_0(e^{j\omega})|^2\frac{G_{uu}(e^{j\omega})}{G_{yg}(e^{j\omega})}. \tag{12}$$

These results apply regardless of the source of $y(k)$. When the linear filter is optimum in the mean-square sense, the error is uncorrelated with $u(k)$, i.e.,

$$G_{ug_0}(e^{j\omega}) = H_0(e^{j\omega})G_{uu}(e^{j\omega}) = G_{uy}(e^{j\omega}). \tag{13}$$

Furthermore, the minimum value of $G_{ee}(e^{j\omega})$ is given by

$$G_{ee}(e^{j\omega}) = G_{yg}(e^{j\omega})[1 - C_{uy}(e^{j\omega})| \tag{14}$$

and

$$G_{y_0y_0}(\omega_n) = |H_0(e^{j\omega})|^2 G_{uu}(e^{j\omega}) = G_{yy}(e^{j\omega})C_{uy}(e^{j\omega}). \tag{15}$$

From the identity

$$G_{yy}(e^{j\omega}) = C_{uy}(e^{j\omega})G_{yy}(e^{j\omega}) + [1 - C_{uy}(e^{j\omega})]G_{yy}(e^{j\omega}) \tag{16}$$

we can show that

$$G_{yy}(e^{j\omega}) = G_{y_0y_0}(e^{j\omega}) + G_{\varepsilon\varepsilon}(e^{j\omega}) \tag{17}$$

indicating that the MSC is the fraction of $G_{yy}(e^{j\omega})$ contained in the linear component of $y(k)$, and $1 - C_{uy}(e^{j\omega})$ is the proportion of $G_{yy}(e^{j\omega})$ contained in the error, or nonlinear component of $y(k)$. These results can be applied to the configuration shown in fig (2)

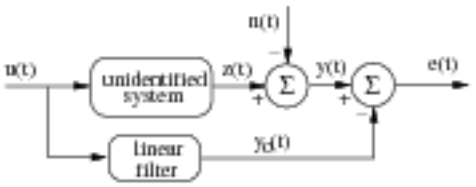


Figure 2: Model of error resulting from linear approximation of unidentified system.

In this paper the coherence spectrum will be used as a measure of confidence of the cross-power spectrum in each frequency ω, this in order to improve the time delay estimation, as shown below in figure (3). In this figure we can see that for low frequencies the coherence spectrum is higher, this is due to the fact that the input and output sequences contain more energy in this frequency range. On the other hand, for higher frequencies the coherence spectrum tends to zero, this is due to the fact that most of the energy in this frequency range comes from the disturbance signal. As a result, we can say that the coherence spectrum can be used to detect in which frequency band the estimation of the cross-power spectrum between the two signals is reliable or not.

Its deviation from one (in some frequency band), among others, can be caused by:

- The spectrum of the disturbance $n(k)$ is large relative to the spectrum of $u(k)$ and $y(k)$.
- The relation between $u(k)$ and $y(k)$ has a strong nonlinear component.

3 Time Delay Estimation For MISO systems

3.1 Delayed Impulse Response for known signals

In this section, we assume that we have an infinite number of sampling data. As mentioned above, a set of p equations is needed to compute the delayed impulse responses, hence, by computing the *Cross-Power Spectrum* (sec. (2.1)) between each input $U(e^{j\omega})$ and the output $Y(e^{j\omega})$ and replacing (5) in (30), this requirement is fulfilled as shown in equation (18).

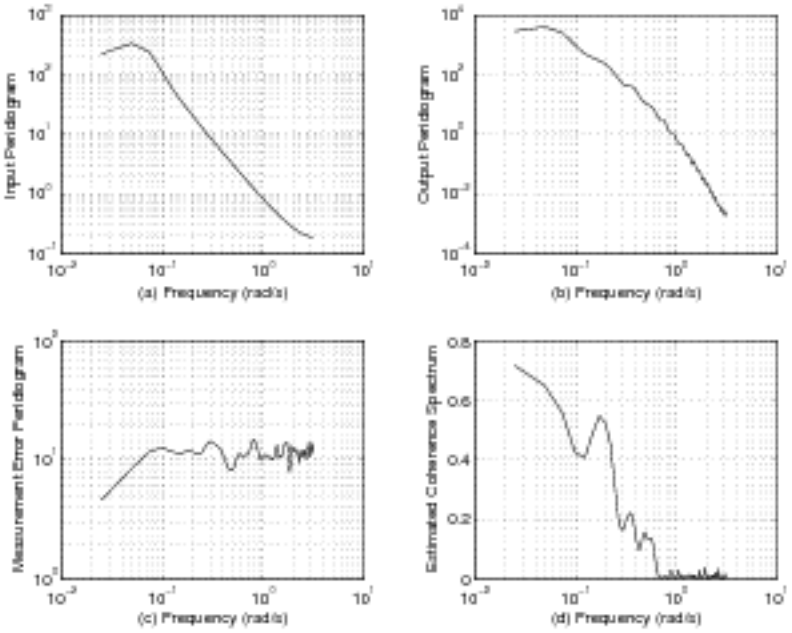


Figure 3: Example of estimated coherence spectrum. (a) Peridiogram of the input signal; (b) Peridiogram of the output signal; (c) Peridiogram of the measurement noise signal; (d) Estimated coherence spectrum.

$$\begin{aligned}
G_{U_1Y}(e^{j\omega}) &= H_1(e^{j\omega})e^{-j\omega\tau_1}U_1(e^{j\omega})U_1^*(e^{j\omega}) + \ldots + H_p(e^{j\omega})e^{-j\omega\tau_p}U_p(e^{j\omega})U_1^*(e^{j\omega}) \\
G_{U_2Y}(e^{j\omega}) &= H_1(e^{j\omega})e^{-j\omega\tau_1}U_1(e^{j\omega})U_2^*(e^{j\omega}) + \ldots + H_p(e^{j\omega})e^{-j\omega\tau_p}U_p(e^{j\omega})U_2^*(e^{j\omega}) \\
\vdots \quad & \quad \vdots \qquad\qquad\qquad\qquad\qquad\qquad \vdots \\
G_{U_pY}(e^{j\omega}) &= H_1(e^{j\omega})e^{-j\omega\tau_1}U_1(e^{j\omega})U_2^*(e^{j\omega}) + \ldots + H_p(e^{j\omega})e^{-j\omega\tau_p}U_p(e^{j\omega})U_p^*(e^{j\omega})
\end{aligned} \tag{18}$$

Then, rewriting (18) in matrix form

$$\underbrace{\begin{bmatrix} G_{U_1Y}(e^{j\omega}) \\ \vdots \\ G_{U_pY}(e^{j\omega}) \end{bmatrix}}_{\boldsymbol{G}_{p\times 1}} = \underbrace{\begin{bmatrix} U_1(e^{j\omega})U_1^*(e^{j\omega}) & \ldots & U_p(e^{j\omega})U_1^*(e^{j\omega}) \\ \vdots & \ddots & \vdots \\ U_1(e^{j\omega})U_p^*(e^{j\omega}) & \ldots & U_p(e^{j\omega})U_p^*(e^{j\omega}) \end{bmatrix}}_{\boldsymbol{A}_{p\times p}} \underbrace{\begin{bmatrix} H_1(e^{j\omega})e^{-j\omega\tau_1} \\ \vdots \\ H_p(e^{j\omega})e^{-j\omega\tau_p} \end{bmatrix}}_{\boldsymbol{H}_{p\times 1}} \tag{19}$$

where $\boldsymbol{A} \in \mathbb{C}^{p\times p}$ is positive definite, and contains the power and cross-power spectrum $U(e^{j\omega})U^*(e^{j\omega}) \in \mathbb{R}$ and $U(e^{j\omega})U_j^*(e^{j\omega}) \in \mathbb{C}$ of the input variables, respectively. $\boldsymbol{G} \in \mathbb{C}^{p\times 1}$ contains the cross-power spectrum between the input i and the output, and $\boldsymbol{H} \in \mathbb{C}^{p\times 1}$ contains the delayed transfers functions $\boldsymbol{H}_i$ between the input i and the output at the frequency ω_j. Consequently, equation (19) can be written in a compact form as

$$\boldsymbol{G} = \boldsymbol{A}\boldsymbol{H} \tag{20}$$

Now, solving equation (20) for $\boldsymbol{H}$ we have

$$\boldsymbol{H} = \boldsymbol{A}^{-1}\boldsymbol{G} \tag{21}$$

this equation is an extension of the Wiener-Hopf filter for MISO systems, where $\boldsymbol{A}$ has to be invertible.

Thus, solving equation (21) the matrix $\boldsymbol{H}$ which contains the delayed impulse responses in the Laplace domain is obtained. Afterwards, the IDTFT is applied to $\boldsymbol{H}$, and the time delays computed, assuming a gaussian distribution, as the point when the impulse response becomes bigger than zero.

4 Problem Formulation

Let us assume that $\boldsymbol{U} \in \mathbb{R}^{N\times p}$, $\boldsymbol{E} \in \mathbb{R}^{N\times 1}$, and $\boldsymbol{Y} \in \mathbb{R}^{N\times 1}$ are measured data sequences consisting of N equidistant time points of an LTI MISO system with p inputs and one output as shown in figure (4)

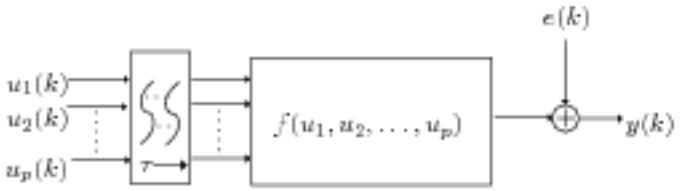


Figure 4: LTI MISO system with p known inputs $u(k)$ with unknown delays, one known output $y(k)$, and the unknown noise signal $e(k)$ which represents the input-output noise measurement, where $f(u_1, u_2, \ldots, u_p)$ is an unknown linear function (i.e., linear dynamic system) of $u(k)$.

such that

$$y(k) = f(u_1(k), u_2(k), \ldots, u_p(k)) + e(k), \quad 0 \leq k \leq N-1, \tag{22}$$

The problem considered here is to estimate the time delays τ between the i_{th} input $u_i(k)$ and the output $y(k)$, taking into account that $y(k)$ is also affected by the other inputs and the noise signal $e(k)$.

Some classical methods like *PHAT, ROTH, SCOT, CRA, Bispectrum* (see [6], [2] for a survey), compute the time delay between two signals, typical input and output, for SISO (Single Input-Single Output) systems by estimating the impulse response based on the Generalized Cross-Correlation function [6], as can be seen in figure (5). Thus, depending on the particular form of the filtering function $\Psi_g(e^{j\omega})$, one can have a different performance of the cross-correlation function. For example, when the role of the filter is to accentuate the signal passed to the correlator at those frequencies at which the signal-to-noise (S/N)

ratio is highest, then $\Psi_g(e^{j\omega})$ can be expected to be a function of signal and noise spectra which must either be known *a priori* o estimated. The selection of $\Psi_g(e^{j\omega})$ to optimize certain performance criteria has been studied by several investigators, here some of the most known are shown:

- CRA (Cross-Correlation)

$$\Psi_{gCRA}(e^{j\omega}) = 1. \tag{23}$$

- ROTH Window

$$\Psi_{gR}(e^{j\omega}) = \frac{1}{\hat{G}_{uu}(e^{j\omega})}, \tag{24}$$

  where $\hat{G}_{uu}(e^{j\omega})$ is the estimated power spectrum of $u(k)$.

- SCOT (Smoothed Coherence Transform)

$$\Psi_{gS}(e^{j\omega}) = \frac{1}{\sqrt{\hat{G}_{uu}(e^{j\omega})\hat{G}_{yy}(e^{j\omega})}}, \tag{25}$$

  where $\hat{G}_{uu}(e^{j\omega})$ is the estimated power spectrum of $x(k)$, and $G_{yy}(e^{j\omega})$ is the estimated power spectrum of $y(k)$.

- PATH (Phase Transform)

$$\hat{\Psi}_{gP}(e^{j\omega}) = \frac{1}{|\hat{G}_{ug}(e^{j\omega}|}, \tag{26}$$

  where $\hat{G}_{ug}(e^{j\omega})$ is the estimated cross power spectrum between $u(k)$ and $y(k)$.

- ML (Maximum Likelihood)

$$\Psi_{gML}(e^{j\omega}) = \frac{1}{|\hat{G}_{ug}(e^{j\omega})|} \frac{|\hat{\gamma}_{ug}(e^{j\omega})|^2}{[1 - |\hat{\gamma}_{uy}(e^{j\omega})|^2]}, \tag{27}$$

  where $\hat{G}_{ug}(e^{j\omega})$ is the estimated cross power spectrum between $u(k)$ and $y(k)$, and $\hat{\gamma}_{uy}(e^{j\omega})$ is the coherence spectrum between $u(k)$ and $y(k)$ (see section (2.2)).

In this paper we will extend these ideas to the MISO system case, assuming the system is linear-time-invariant (LTI), and taking into account that the input and output signals are coupled.

Therefore, given the system shown in figure (6), where $U_1(s), U_2(s), ..., U_p(s)$, $Y(s)$, and $E(s)$ are respectively input, output, and noise variables in the Laplace domain, and a set of unknown transfer functions $H_i(s)$ from each input i to the output. Thus, $Y(s)$ can be written as

$$Y(s) = H_1(s)U_1(s) + H_2(s)U_2(s) + \ldots + H_p(s)U_p(s) + E(s). \tag{28}$$

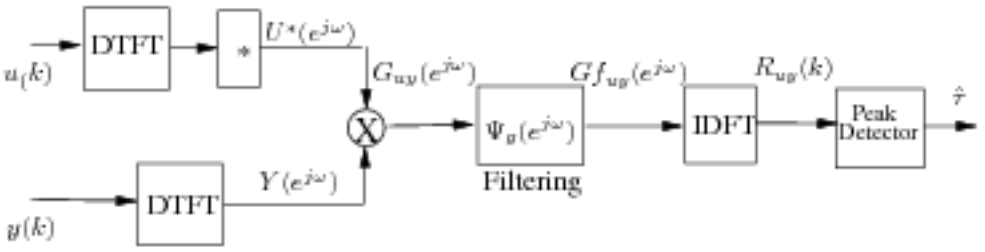


Figure 5: Time delay estimation for SISO systems based on the generalized cross-correlation. Where $u(k)$ and $y(k)$ are the input and output signal respectively, $G_{uy}(e^{j\omega})$ is the cross-power spectrum between the input and output signals, $\Psi_g(e^{j\omega})$ is a filtering function that depends on the method to be used to make the time delay estimation such as CRA, PATH, ROTH, SCOT or ML. $Gf_{uy}(e^{j\omega})$ is the filtered cross-power spectrum after passing by $\Psi_g(e^{j\omega})$, $R_{ug}(k)$ is the filtered cross-correlation between $u(k)$ and $y(k)$, and finally $\hat{\tau}$ is the time delay estimation.

Now, defining the time delay between input i and the output, as τ, (see figure (6)), equation (28) can be rewritten as

$$Y(s) = H_1(s)e^{-\tau_1 s}(s)U_1(s) + \ldots + H_p(s)e^{-\tau_p s}U_p(s) + E(s), \qquad (29)$$

or, evaluated on the imaginary axis, per frequency

$$Y(e^{j\omega}) = H_1(e^{j\omega})e^{-j\omega\tau_1}U_1(e^{j\omega}) + \ldots + H_p(s)e^{-j\omega\tau_p s}U_p(s) + E(s), \qquad (30)$$

with $\omega = wT$, where T is the sampling time and $w \in \mathbb{R}$ the angular frequency.

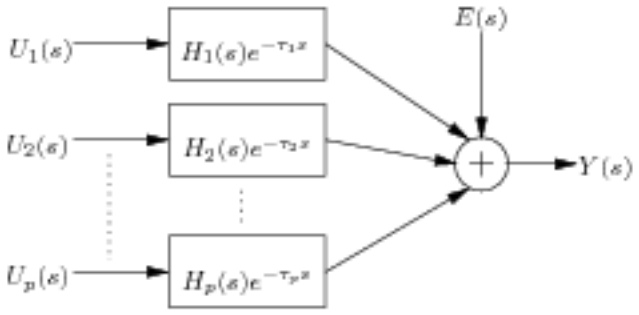


Figure 6: LTI MISO delayed system in Laplace domain. with $U(s)$, $Y(s)$, and $E(s)$ the input, output and measurement noise variables in the Laplace domain respectively. $H_i(s)e^{-}$ the delayed transfer function from the i_{th} input to the output.

As a result, the delayed impulse responses $H_1(e^{j\omega})e^{-j\omega\tau_1}$, $H_2(e^{j\omega})e^{-j\omega\tau_2}$, $\ldots$, $H_p(e^{j\omega})e^{-j\omega\tau_p}$ can be computed from the cross-correlation function between input and output signals, as shown in section 2.1.

4.1 Regularized Time Delay Estimation (RTDE)

In the previous section the analysis was done based on Discrete Time Fourier Transform, however, to compute this signal transform we need information of the signal in time from $-\infty$ to ∞. Nevertheless, in practice, we only have access to a finite number of data samples. For this class of sequences $x(k)$, the Discrete-Fourier Transform (DFT) is defined as

$$X_N(\omega_n) = \sum_{n=0}^{N-1} x(k) e^{-j\omega_n kT}, \tag{31}$$

for $\omega_n = \frac{2\pi n}{NT}, n = 0, 1, 2, \ldots, N-1$ and sampling time T.

Now, replacing the $DTFT$ by DFT in (12), (13), (14) we have

$$\underbrace{\begin{bmatrix} \hat{G}_{U_1 Y}(\omega_n) \\ \vdots \\ \hat{G}_{U_p Y}(\omega_n) \end{bmatrix}}_{\hat{\boldsymbol{G}}_{p\times 1}} = \underbrace{\begin{bmatrix} \hat{U}_1(\omega_n)\hat{U}_1^*(\omega_n) & \ldots & \hat{U}_p(\omega_n)\hat{U}_1^*(\omega_n) \\ \vdots & \ddots & \vdots \\ \hat{U}_1(\omega_n)\hat{U}_p^*(\omega_n) & \ldots & \hat{U}_p(\omega_n)\hat{U}_p^*(\omega_n) \end{bmatrix}}_{\hat{\boldsymbol{A}}_{p\times p}} \underbrace{\begin{bmatrix} \hat{H}_1(\omega_n)e^{-j\omega_n\tau_1} \\ \vdots \\ \hat{H}_p(\omega_n)e^{-j\omega_n\tau_p} \end{bmatrix}}_{\boldsymbol{H}_{p\times 1}} + \ldots + \underbrace{\begin{bmatrix} V_1(\omega_n) \\ \vdots \\ V_p(\omega_n) \end{bmatrix}}_{\boldsymbol{V}_{p\times 1}}, \tag{32}$$

where $\hat{\boldsymbol{A}} \in \mathbb{C}^{p\times p}$ is positive definite, and contains the estimated power and cross-power spectrum $U(e^{j\omega})U^*(e^{j\omega}) \in \mathbb{R}$ and $U(e^{j\omega})U_j^*(e^{j\omega}) \in \mathbb{C}$ of the input variables, respectively. $\hat{\boldsymbol{G}} \in \mathbb{C}^{p\times 1}$ contains the estimated cross-power spectrum between the input i and the output, $\boldsymbol{H} \in \mathbb{C}^{p\times 1}$ contains the delayed transfers functions $H_i(\omega_n)$ between the i_{th} input $u_i(k)$ and the output $y(k)$ at the frequency ω_j, and $\boldsymbol{V}$ is the unknown cross-power spectrum between the measurement error and $u_i(k)$. As a result, equation (32) can be written as [1]

$$\hat{\boldsymbol{G}} = \hat{\boldsymbol{A}}\boldsymbol{H} + \boldsymbol{V}. \tag{33}$$

On the other hand, since the MSC $C_{u_i y}(\omega_n)$ gives information about how reliable the cross-power spectrum $G_{u_i y}(\omega_n)$ is at certain frequencies ω_j, this will be used as a weighted parameter in the solution of equation (33). Consequently, the problem can be formulated as an RLS (Regularized Least Squares) problem, as follows:

$$\min_{\boldsymbol{H}} \|\hat{\boldsymbol{A}}\boldsymbol{H} - \hat{\boldsymbol{G}}\|_2^2 + \lambda^2 \|\boldsymbol{L}\boldsymbol{H}\|_2^2, \tag{34}$$

[1] The estimation of the cross and power spectrum in equation (32) is made based on P. Welch's method (Peridiograms) [7].

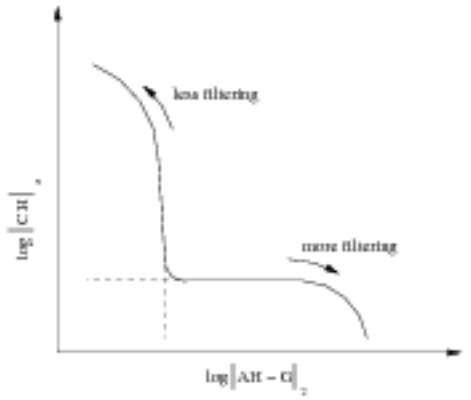


Figure 7: The generic form of the L-Curve

where $\boldsymbol{L} = \boldsymbol{I} - \boldsymbol{C}$, $\boldsymbol{I} \in \mathbb{R}^{p \times p}$ is the identity matrix, and $\boldsymbol{C} \in \mathbb{R}^{p \times p}$ is defined as

$$\boldsymbol{C} = diag(|C_{u_1 y}(\omega_j) \ldots C_{u_p y}(\omega_j)|), \tag{35}$$

a diagonal matrix containing the coherence spectrums at the frequency ω_j, and λ is a regularization parameter that must be chosen such that the solution of equation (34) $\boldsymbol{H}$, is a compromise between the minimization of $\|\hat{\boldsymbol{A}}\boldsymbol{H} - \hat{\boldsymbol{G}}\|_2$ and $\lambda\|\boldsymbol{L}\boldsymbol{H}\|_2$ (see [5], [4]). A large λ (equivalent to a large amount of regularization) favors small solution seminorm at the cost of a large residual norm, while a small λ (i.e., a small amount of regularization) has the opposite effect. Also can be shown that λ controls the sensitivity of the regularized solution $\boldsymbol{H}$ to perturbation in $\hat{\boldsymbol{A}}$ and $\hat{\boldsymbol{G}}$, and the perturbation bound is proportional to λ^{-1}. Thus, the regularization parameter λ is an important quantity which controls the properties of the regularized solution, and λ should therefore be chosen with care.

One very well-known method to compute λ is the *L-Curve* which is a plot -for all valid regularization parameters- of the (semi)norm $\|\boldsymbol{L}\boldsymbol{H}\|_2$ of the regularized solution versus the corresponding residual norm $\|\hat{\boldsymbol{A}}\boldsymbol{H} - \hat{\boldsymbol{G}}\|_2$. In this way, the *L-Curve* clearly displays the compromise between minimization of these two quantities, which is the heart of any regularization method (see figure (7)).

Then, after choosing λ in accordance to the *L-Curve* method, the minimization problem described in equation (34) is solved using the Tikhonov regularization approach (see [5] for details).

The Tikhonov's method computes the regularized solution $\boldsymbol{H}$ of equation (34) as the solution to the following least squares problem

$$min \left\| \begin{pmatrix} \hat{\boldsymbol{A}} \\ \lambda^{1/2}\boldsymbol{L} \end{pmatrix} \boldsymbol{H} - \begin{pmatrix} \hat{\boldsymbol{G}} \\ \boldsymbol{0} \end{pmatrix} \right\|_2^2, \tag{36}$$

that is equivalent to the solution of

$$(\hat{\boldsymbol{A}}^{\boldsymbol{T}}\hat{\boldsymbol{A}} + \lambda \boldsymbol{L}^{\boldsymbol{T}}\boldsymbol{L})\boldsymbol{H} = \hat{\boldsymbol{A}}^{\boldsymbol{T}}\hat{\boldsymbol{G}}. \tag{37}$$

Finally, the IDFT is applied to $\boldsymbol{H}$ in order to find the estimated delayed impulse responses in the time domain. Then, the time delays are obtained by looking at the maximum values of the estimated impulse responses.

5 Numerical Results

In this section we will compare RTDE with the classical non-parametric methods, PATH, ROTH, SCOT and ML, for a MISO system with four inputs, one output, and different values of SNR.

To make the simulations four delayed linear systems were selected

$$G_1(s) = \frac{e^{-5s}}{(s+0.7)(s+0.5)} \quad G_2(s) = \frac{e^{-20s}}{(s+0.8)(s+1.3)}$$

$$G_3(s) = \frac{e^{-9s}}{(s+0.3)(s+1.8)} \quad G_4(s) = \frac{e^{-13s}}{(s+0.5)(s+1.5)} \tag{38}$$

with their respective time delays:

$$\tau_1 = 5\,sec, \quad \tau_2 = 20\,sec, \quad \tau_3 = 9\,sec, \quad \tau_4 = 13\,sec$$

Initially four different step piece-wise input signals of length 4850 were generated, assuming a sampling time of 1 second (see figure (8)). Then, in order to investigate the performance of RTDE for different conditions of noise, uncorrelated white noise, uncorrelated coloured noise and correlated coloured noise were added to the original input and output signals. The computations and simulations were made in Matlab 6.5.

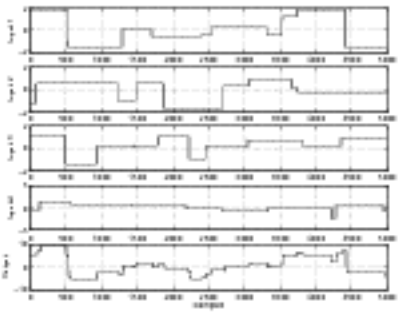


Figure 8: Input-Output signals without noise of the MISO system with 4 inputs, 1 output. The input signals were generated randomly. Each data set contains 4850 samples, with a sampling time of 1 second.

5.1 Case A: Inputs and Output Signals without Measurement Noise

Four random step piece-wise input signals were generated as shown in figure (8). Then, by choosing a window of 128 samples, the time delay estimation for the methods mentioned above were carried out.

Table (1) shows that the performance of the methods is very good when the input and output signals are no corrupted with noise. Moreover, as can be seen in figure (9), the estimations are very reliable, due to fact that the plots show a very clear peak at the corresponding time delay.

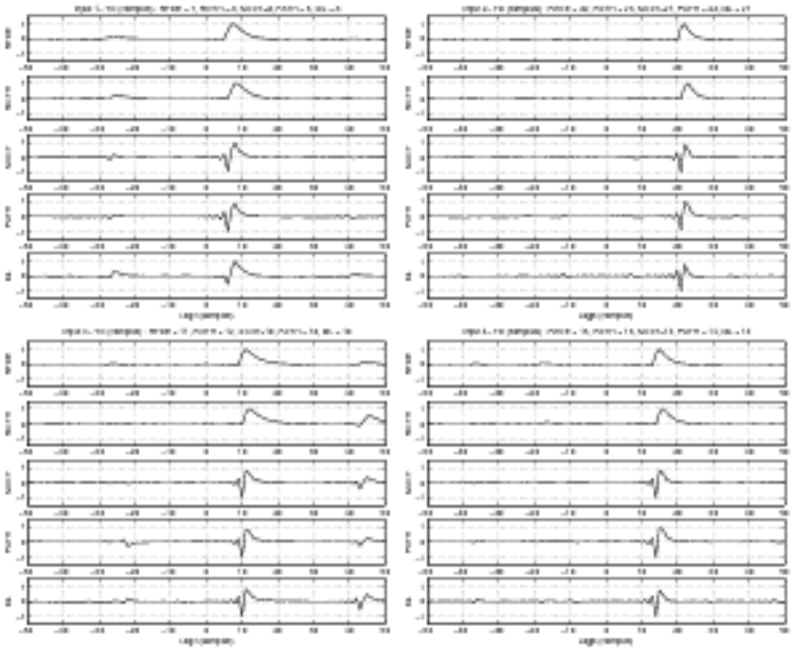


Figure 9: Time delay estimation - Input-Output signals without noise. Comparison of delayed impulse responses estimation between RTDE to classical cross-correlation methods.

Inputs (samples)	RTDE	ROTH	SCOT	PATH	ML
$u_1/error$	7/2	8/3	8/3	6/1	8/3
$u_2/error$	22/2	23/3	21/1	22/2	21/1
$u_3/error$	11/2	12/3	10/1	10/1	10/1
$u_4/error$	15/2	16/3	14/1	14/1	14/1

Table 1: Time delay estimation - Input-Output signals without noise.

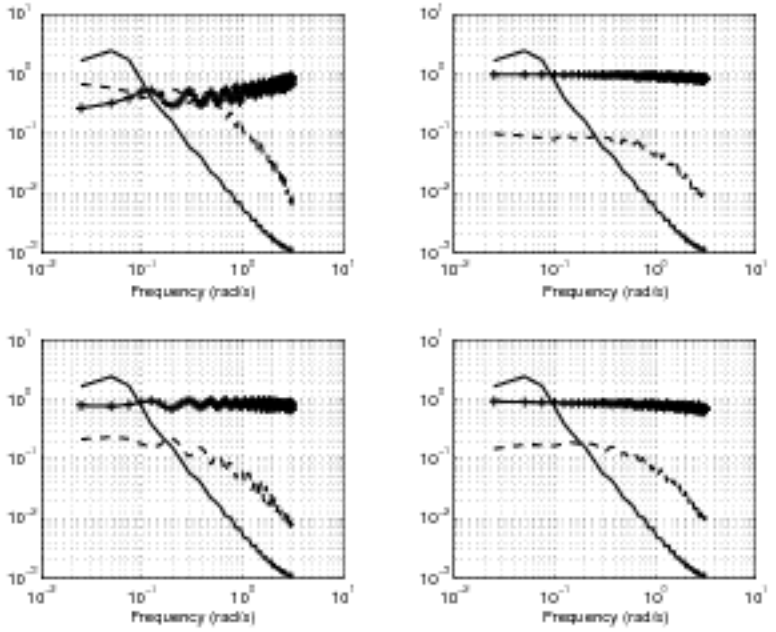


Figure 10: Comparison between $L = 1 - C_{\alpha,\beta}(\omega_n)$ (plus line), $H_{u_i y}(\omega_n)$ (dashed line), and the regularized parameter $\lambda/100$ (solid line). In this plot can be seen that L is a smaller than one for low frequencies, and very closed to one for high frequencies, it means, that most of the energy of the signals is located at low frequencies, this is due to the frequency bandwidth of system itself. Hence, λ takes bigger values for low frequencies, making the regularized term $\lambda \| L\boldsymbol{H} \|_2^2$ rejected in the minimization, and low values for high frequencies making the regularized term included in the minimization.

5.2 Case B: Inputs and Output Signals with Uncorrelated White Measurement Noise

The Gaussian noise signals were generated using different seeds with the command *randn* of Matlab to guarantee their independence. Then, they were added to the original ones in order to analyze the performance of the methods under this conditions. In general, table (2) shows that RTDE performs better and more

Inputs (samples)	RTDE	ROTH	SCOT	PATH	ML	SNR (dB)
$u_1/error$	7/2	9/4	8/3	8/3	9/4	13
$u_2/error$	21/1	9/11	9/11	9/11	9/11	9.5
$u_3/error$	11/2	16/7	16/7	16/7	16/7	8.3
$u_4/error$	16/3	17/4	17/4	17/4	16/3	8.1

Table 2: Time delay estimation - Uncorrelated white noise.

reliable than the others under white noise conditions, this is due to the regularized parameters that depend of the coherence spectrum, as a result, RTDE is more robust against white noise measurements, as can be seen in figure (12)

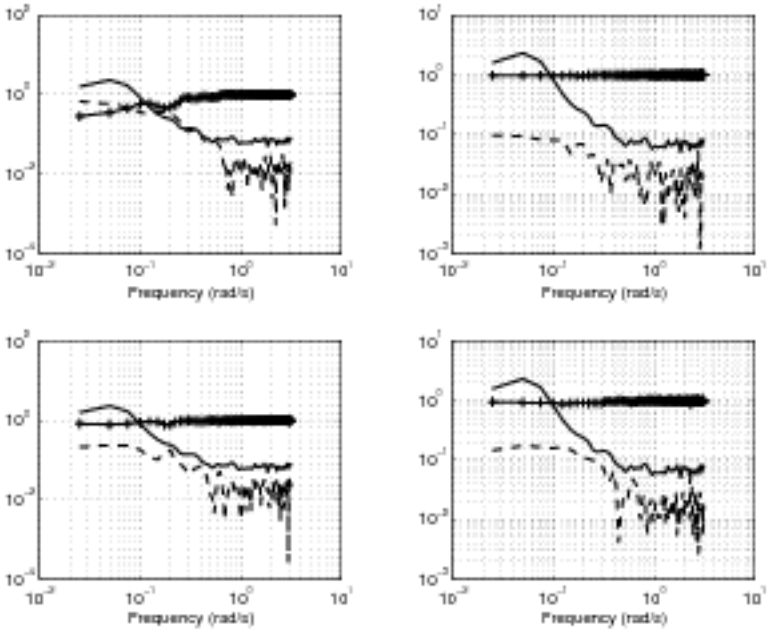


Figure 11: Comparison between $L = 1 - C_{u;y}(\omega_n)$ (plus line), $H_{u;y}(\omega_n)$ (dashed line), and the regularized parameter $\lambda/100$ (solid line). For this case is observed clearly that for high frequencies L rises to one, due to the fact that the information located there is originated for the measurement noise signal. Therefore RTDE behaves as a low-pass filter, but at the same time λ does no drop too much in this frequency bandwidth, it means that the regularized term $\mathrm{L}\boldsymbol{H}\|_2^2$ is involved in the minimization, making the estimation more robust.

5.3 Case C: Inputs and Output Signals with Uncorrelated Coloured Measurement Noise

The uncorrelated Gaussian noise signal were generated using the different seeds with the command *randn* of Matlab to guarantee their independence, and then filtered with a high-pass butterworth filter of fourth order, with cutoff frequency of 0.3 times the nyquist frequency. Then, they were added to the original ones, in order to analyze the performance of the methods under this conditions. In

Inputs (samples)	RTDE	ROTH	SCOT	PATH	ML	SNR (dB)
$u_1/error$	10/5	11/6	11/6	11/6	10/5	1.9
$u_2/error$	20/0	21/1	9/11	9/11	9/11	1
$u_3/error$	15/6	16/7	16/7	16/7	16/7	0.73
$u_4/error$	18/5	19/6	19/6	19/6	19/6	0.72

Table 3: Time delay estimation - Uncorrelated coloured noise

general, table (3) shows that the performance of RTDE is again better than the other methods. On the other hand SCOT, PATH, and ML fail to detect the delay in the second input due to the fact that the coloured noise is not filtered

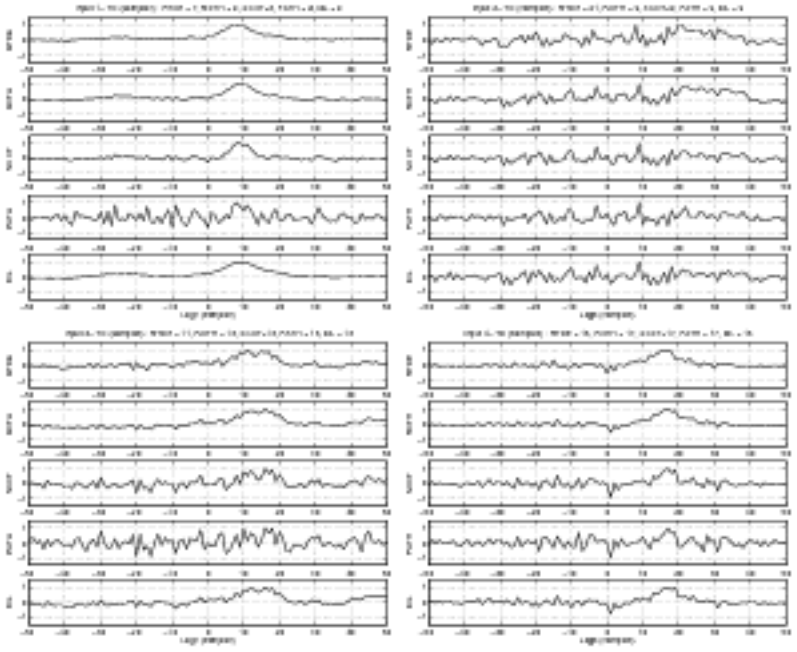


Figure 12: Time delay estimation - Uncorrelated white noise. Comparison of delayed impulse responses estimation between RTDE to classical cross-correlation methods.

causing a perturbation in the estimation. Also, in figure (13) can be seen that the impulse response estimations are very smooth in most of the cases, therefore, we can say that the results are very reliable.

5.4 Case D: Inputs and Output Signal with Correlated Coloured Measurement Noise

The correlated Gaussian noise signal were generated using the same seed with the command *randn* of Matlab to guarantee their dependence. Then, they were added to the original ones, in order to analyze the performance of the methods under this conditions.

Inputs (samples)	RTDE	ROTH	SCOT	PATH	ML	SNR (dB)
$u_1/error$	8/3	9/4	9/4	9/4	6/1	3.7
$u_2/error$	22/2	23/3	6/14	23/3	4/16	2.1
$u_3/error$	12/3	13/4	13/4	13/4	10/1	1.6
$u_4/error$	15/2	17/4	17/4	17/4	14/1	1.5

Table 4: Time delay estimation - Correlated coloured noise. Estimation are taken after the first lag.

Table (4) shows that most of the methods can make a good estimation, except for SCOT in the second and third input, and ML in the first input.

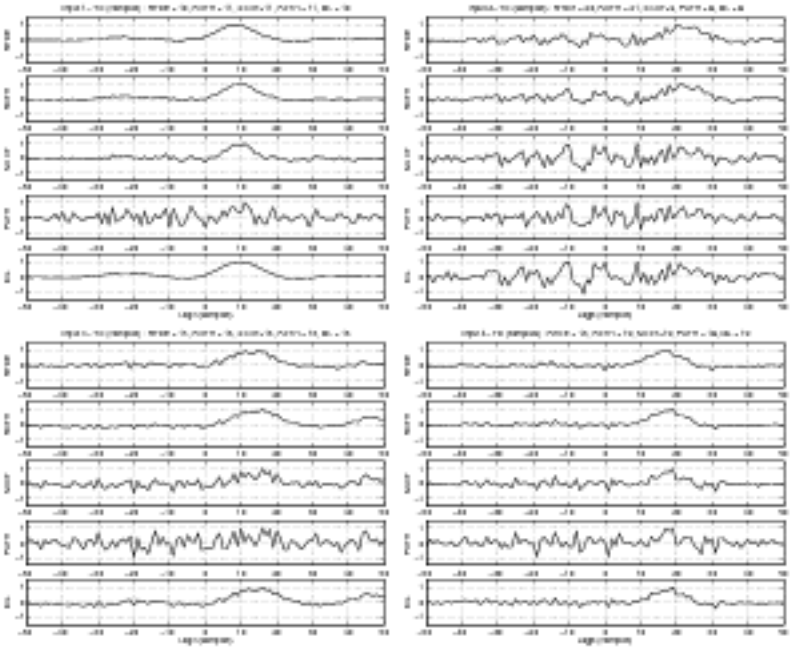


Figure 13: Time delay estimation - Uncorrelated coloured noise. Comparison of delayed impulse responses estimation between RTDE to classical cross-correlation methods.

However, in figure (16) can be observed that RTDE works pretty well compare to the others, because it is not affected as the rest for the correlated noise inputs, due to the regularized parameters of the RLS solution. As can be seen in figure (16) around zero there is a peak which is caused by the noise correlation, as a consequence, for classical methods we have to take into account this fact, and look for the maximum value far away of zero. However, RTDE seems to be very robust due to the fact that in the most cases (except for the input 2) the peak caused by the time delay is bigger than the peak caused by the noise correlation.

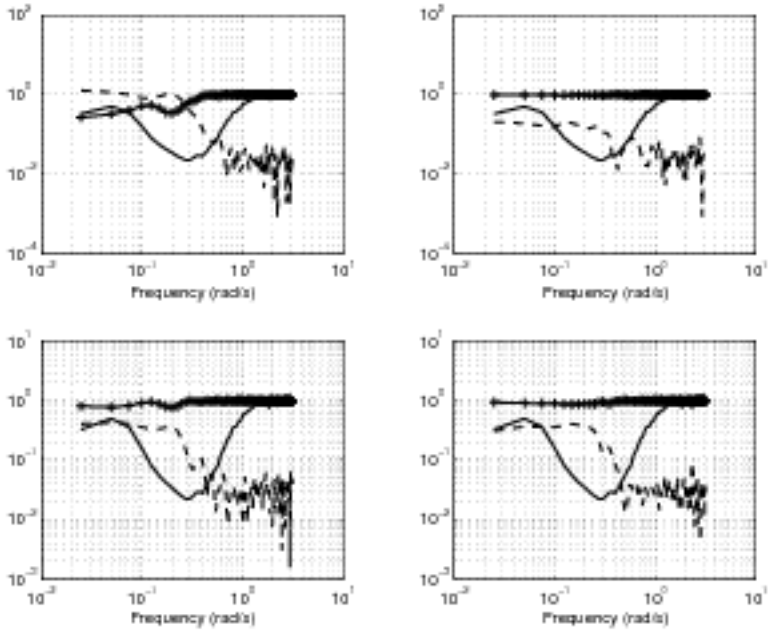


Figure 14: Comparison between $L = 1 - C_{\alpha,\beta}(\omega_n)$ (plus line), $H_{u,y}(\omega_n)$ (dashed line), and the regularized parameter $\lambda/100$ (dashed line). In this figure is seen how λ reacts when the coloured noise is detected penalizing the regularized term with a high weighting value.

6 Conclusions

In this paper we have introduced a new non-parametric approach, RTDE. This approach has shown to be more realiables than the classical ones, for the MISO systems case in very critical noise conditions. By using the information that the coherence spectrum gives about the reliability of the cross-power spectrum, the problem of time delay estimation can be formulated as a RLS problem. Due to the RLS formulation we can have a very robust estimator in the sense of better performance under problems of noise input correlation and noisy signals.

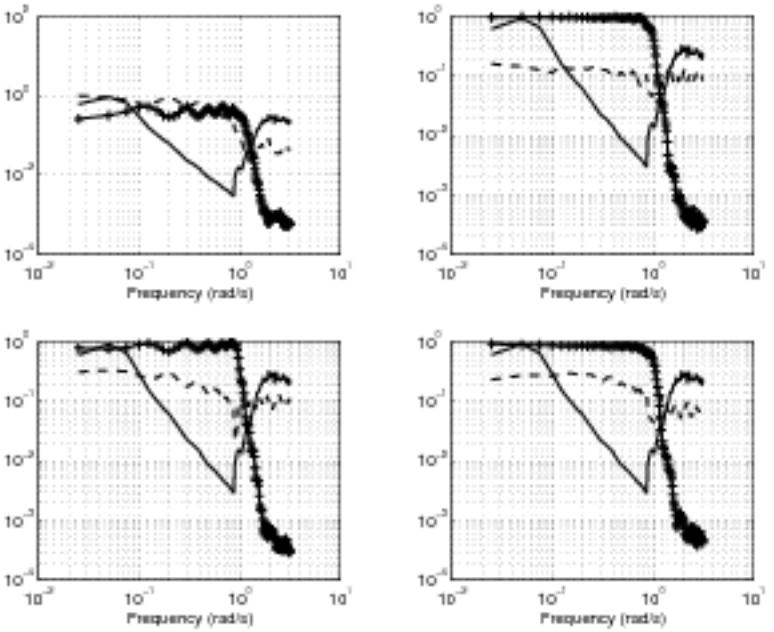


Figure 15: Comparison between $L = 1 - C_{u;y}(\omega_n)$ (plus line), $H_{u;y}(\omega_n)$ (dashed line), and the regularized parameter $\lambda/100$ (solid line). In this figure we can see that the coherence spectrum fails in detecting the noise signal, this is why always appears a peak in the zero lag, but on the other hand, RTDE and the other methods keep the information of the low frequencies, making the estimation still possible. Spite of this, RTDE is able to detect the delay in the first and third inputs.

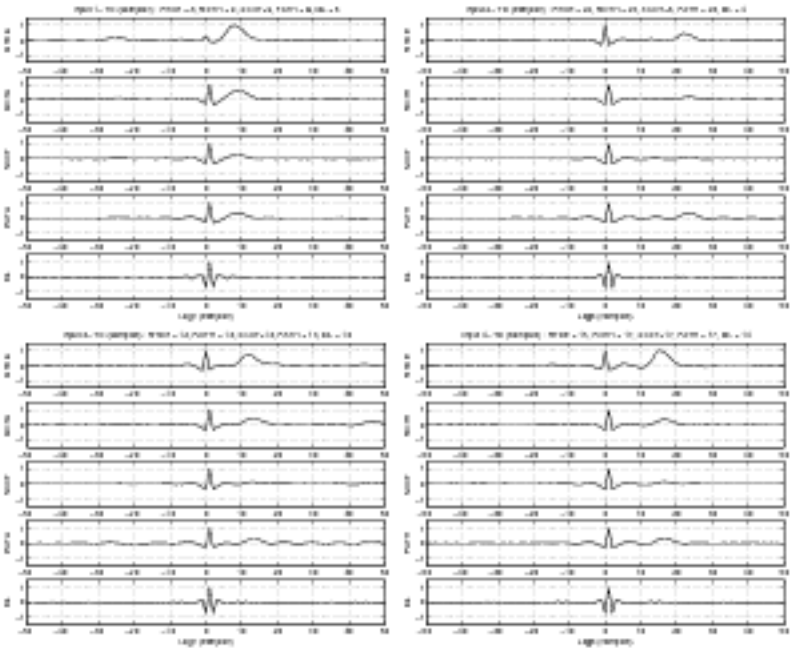


Figure 16: Time delay estimation - Correlated coloured noise. Comparison of delayed impulse responses estimation between RTDE to classical cross-correlation methods.

References

[1] M.R. Raghuveer C. Nikias. Bispectrum estimation: A digital signal processing framework. *Proceedings of the IEEE*, 75(7), july 1987.

[2] R. Pan C. Nikias. Time delay estimation in unknown gaussian spatially correlated noise. *IEEE Trans. on Acoustics, speech, and signal processing*, 36(11), November 1988.

[3] G.C. Carter. Coherence and time delay estimation. *Proceedings of the IEEE*, 75(2), February 1987.

[4] C. Hansen G. Golub and P. O'Leary. *Tikhonov Regularization and Total Least Squares*. Stanford University, 1998. Technical Report SCCM-98-10.

[5] C. Hansen. *Regularization Tools: A Matlab Package for Analysis and Solution of Discete Ill-Posed Problems*. Technical University of Denmark, Dept. of Mathematical Modelling, 2001.

[6] C. Knapp and C. Clifford. The generalized correlation method for estimation of time delay. *IEEE Trans. on Acoustics, Speech, and Signal Proc.*, ASSp-24(4), Aug. 1976.

[7] Welch Peter. The use of fast fourier transform for the estimation of power spectra: A method based on time averaging over short, modified peridograms. *IEEE trans. Audio and Electroacoust.*, AU-15:70–73, 1967.